Preparation and Characterization of Interfacially Polymerized Polyamide Membrane for Dye Removal

Nurul F. Himma*, Bambang Ismuyanto, A.S. Dwi Saptati N.H., Juliananda, Hidayatul M. Rohmawati, Irfan Budiarta

Department of Chemical Engineering, Faculty of Engineering, Universitas Brawijaya,
Jl. Mayjen Haryono 167 Malang, 65145, Indonesia
*E-mail: nfhimma@ub.ac.id

Abstract

Dye removal from wastewater is one of the major environmental concerns, and membrane-based separation has gained great attention as a promising technology to remove dyes effectively and efficiently. However, membrane development is still necessary to obtain a high-performance membrane. In this work, interfacial polymerization of polyamide was conducted using hydrophobic and hydrophilic membrane support to obtain thin-film composite membranes. The effects of monomer concentration were investigated, and the resulting thin-film composite membranes were tested for their performance in dye removal using different flow configurations. The results showed that a dense polyamide layer was successfully formed on the hydrophilic support, while a polyamide layer with a very loose structure was formed on the hydrophobic support. The polyamide layer became smoother and more hydrophilic as the concentration of trimesoyl chloride was increased, leading to increased permeate flux and reduced dye rejection. The highest sunset yellow rejection of 45.7% with a permeate flux of 4.9 L/m^2.h was obtained when the polyamide layer was formed from trimesoyl chloride concentration of 0.05 w/v% (a high amine to acid chloride monomer ratio of 20) and the filtration was in cross-flow configuration.

Keywords: dye removal; interfacial polymerization; polyamide; sunset yellow; thin-film composite membrane

1. Introduction

Synthetic dyes are widely used in the textile, paper, paint, food, pharmaceutical, and cosmetics industries. Releasing untreated or poorly treated wastewater from these industries into the water bodies leads to problems in aquatic ecosystems, which reduces light penetration in water causing changes in photosynthetic activity then affects the aquatic biota. Besides, the use of water contaminated with dyes can cause cancer and organ malfunctions. Therefore, the removal of dyes from the wastewater becomes a major environmental concern (Katheresan et al., 2018; Samsami et al., 2020; Kustiningsi et al., 2020).

A number of physical and chemical methods have been developed and used for wastewater treatment, including coagulation, adsorption, and electrochemical processes (Collivignarelli et al., 2019). In coagulation, a large amount of coagulant is required for highly colored wastewater, resulting in a large amount of chemical sludge. When using adsorption, regeneration of the adsorbent is often undesired since it is generally inefficient

and expensive. Electrochemical processes could effectively remove the contaminants without generating large sludge, but its application for real scale is challenging. Membrane technology is an emerging separation method that provides many advantages over conventional technologies, such as feasible for continuous operation and scale-up, low energy consumption, and environmentally friendly.

A membrane process that is suitable for dye removal is nanofiltration. It is a pressure-driven membrane technology that is able to separate most organic solutes with molecular weights above 150–2000 Da (Paul and Jons, 2016). Nanofiltration membrane is commonly made from polymeric materials because they are easier to process compared to inorganic materials such as ceramics. In membrane development for nanofiltration, interfacial polymerization (IP) method has received a lot of attention since it is able to produce a composite membrane with a thin and selective top layer (Mohammad et al., 2015; Paul and Jons, 2016).

Several studies have been conducted to optimize selective layer formation. Several studies (Esfandian et al., 2017; Yan et al., 2019) used more polar solvents in the organic phase, called co-solvent-assisted IP, to increase the monomer solubility from the aquatic phase to the organic phase, producing thinner and denser layer. Their membranes were then used for lactose recovery (Esfandian et al., 2017) and desalination (Yan et al., 2019). In addition to the solution system, the support membrane is also an important factor affecting the selective layer formation. In this regard, porous membranes made from hydrophilic or slightly hydrophobic polymers such as polyacrylonitrile (PAN) (Park et al., 2018; Zhu et al., 2018), polyethersulfone (PES) (Shen et al., 2016), and polysulfone (PSF) (Yan et al., 2019) are commonly used as the support. A few studies reported the use of hydrophobic membranes for the support (Tian et al., 2013; Zhang et al., 2020). In this work, polyamide (PA) was interfacially polymerized onto porous support membranes with different surface wettability. The effects of acid chloride monomer concentration on the membrane surface morphology and hydrophilicity were investigated, followed by separation tests in dye removal.

2. Methodology

2.1. Materials

Polyethersulfone (PES) and poly(vinylidene fluoride) (PVDF) flat sheet membrane with the same pore size of 0.1 µm from Membrane Solutions, China were used as the hydrophilic and hydrophobic support, respectively. m-phenylenediamine (MPD, flakes, 99%) and 1,3,5-Benzenetricarbonyl trichloride (TMC, 98%) from Sigma-Aldrich were used as monomers for the IP reaction. Hexane from Merck was used as a solvent for the organic phase, while distilled water was used for the aqueous phase. Sunset yellow (90%) with a molecular weight of 452.37 g/mol from Sigma-Aldrich was used as the solute for the separation test.

2.2. Composite Membrane Preparation

A thin PA layer was prepared through IP reaction between MPD and TMC. First, the support membrane was fixed between a plate and gasket–frame assembly. An aqueous solution of MPD was poured onto the membrane surface in the frame. After three minutes of contacting the MPD solution with the support membrane, the residual solution was removed by disassembling the frame and then rolling a rubber roller across the membrane surface. Subsequently, the frame was fixed again on the support membrane. An organic solution (n-hexane) containing TMC was then poured into the frame. After one minute of contact time for PA layer formation, the residual solution was removed. The membrane surface was then rinsed using n-hexane and dried at ambient conditions for 30 minutes. The concentration of MPD was fixed at 1 w/v%, while the concentration of TMC was varied from 0.05 to 0.2 w/v%, corresponding to monomer ratio (MPD/TMC) of 20 to 5. The resulting composite membranes were then coded according to the support and TMC concentration used, i.e. PA/PES M1Tx or PA/PVDF M1Tx, in which x is the TMC concentration.

2.3. Membrane Characterization

Surface morphology of pristine membrane (PES and PVDF support membrane) and PA layer in the composite membrane was obtained by using a scanning electron microscope (SEM, JEOL-JSM-6510LV). The chemical structures were analyzed by using Fourier transform infrared (FTIR, Spectrum Two, PerkinElmer).

The hydrophilicity of the membrane surface was determined by measuring water contact angle (WCA) using a static sessile drop method. A water droplet was put on the membrane surface using a syringe, and the image was captured using a digital microscope. The contact angle was then measured using an image processing and analysis software (ImageJ with Contact Angle plug-in). For each membrane, at least five measurements at different locations were performed to obtain the average contact angle.

2.4. Separation Tests

Before separation tests, pure water flux of the membrane was determined by measuring the volume of pure water (L) over time t (h) for an effective membrane area A (m^2) (Eq. 1).

$$J = \frac{V}{At} \qquad (1)$$

To test the membrane performance, nanofiltration experiment was carried out using an aqueous solution containing sunset yellow at a concentration of 100 ppm as the feed solution. The nanofiltration was conducted in dead-end and cross-flow configuration. All experiments were

conducted at a pressure of 3 bar using a membrane with an effective area of 37.2 cm^2. The permeate flux was then determined by using Eq.1 Meanwhile, the rejection is defined as Equation 2.

$$R = \left(1 - \frac{C_p}{C_f}\right) \times 100\% \qquad (2)$$

where C_f and C_p are concentration of sunset yellow in feed (ppm) and permeate (ppm), respectively, which were measured using UV-Vis spectroscopy at a maximum wavelength of 482 nm. The experiment was conducted three times to ensure reproducibility.

3. Results and Discussion

### 3.1. Surface Morphology and Chemical Structure

The surface morphological changes of the membranes are shown in Figure 1. As shown in Figure 1a, a smooth surface with macropores was obviously observed in the pristine PES membrane. Meanwhile, the PA/PES membranes had a dense structure and a rough surface with ridge-and-valley morphology, which is the typical morphology of PA film obtained from IP reaction. Thus, the distinct surface morphology in the composite membranes confirmed that PA film was successfully formed.

PA/PES membrane obtained from IP reaction between MPD and TMC at a concentration of 1 w/v% and 0.05 w/v%, respectively, had a much rougher surface to the pristine PES membrane (Figure 1b). As the TMC concentration was increased to 0.2 w/v%, the PA layer was smoother (Figure 1c-d). This could be because the PA film is hindered to grow thicker with the high TMC concentration in the reaction zone (Xie et al., 2012), and the crosslinking degree of the PA layer is reduced with the decrease in MPD/TMC ratio (Tian et al., 2013).

While dense PA layer with rough surface evenly covered the PES support membrane, a much looser PA layer was observed when PVDF membrane was used as the support (Figure 1e and f). This could be due to the hydrophobicity of the PVDF membrane hindering the MPD solution to wet the support surface. Since the MPD molecules were not evenly distributed on the support surface, the IP reaction was less developed in some locations, leaving large holes. Besides, the PVDF membrane was much more porous which could be unfavorable for the IP process. Having such morphology, the PA/PVDF membrane was then not tested in separation performance.

The chemical structure of pristine PES and PA/PES membrane was analyzed by FTIR spectra, as presented in Figure 2. The FTIR spectrum of pristine PES membrane shows peaks in the wavenumber of 1579 cm^{-1}, 1487 cm^{-1}, and 1412 cm^{-1}, indicating the presence of aromatic rings (Alenazi et al., 2018; Coates, 2006; Mohamed et al., 2017).
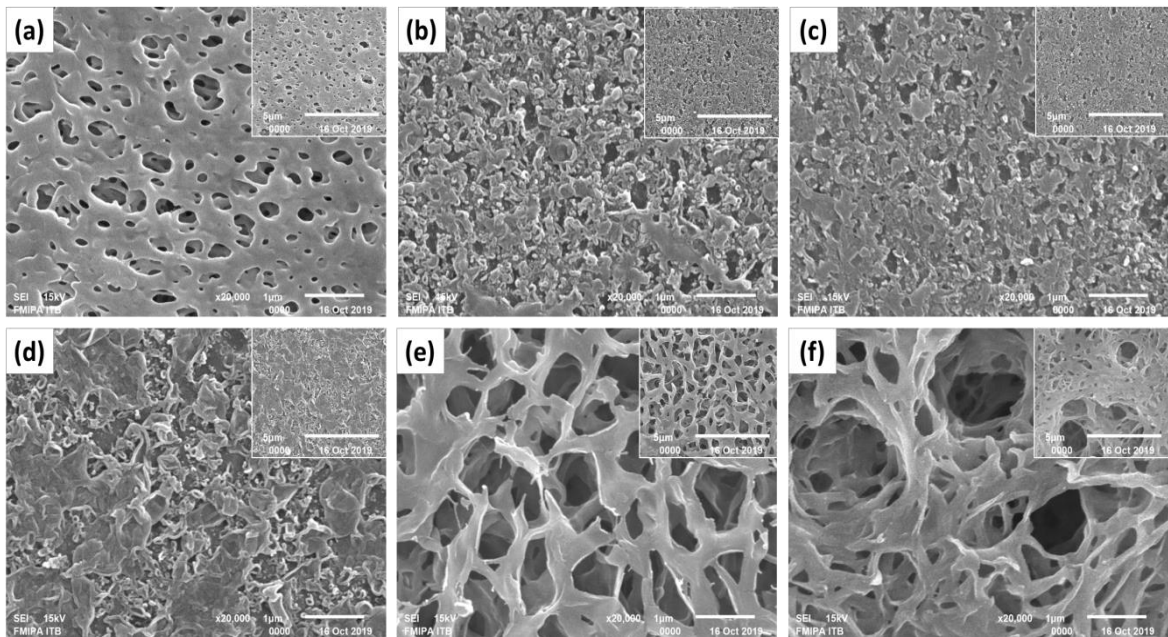
Figure 1. SEM images of membrane surface: (a) PES, (b) PA/PES M1T0.05, (c) PA/PES M1T0.1 (d) PA/PES M1T0.2, (e) PVDF, and (f) PA/PVDF M1T0.1. The inset figures are their SEM images with a smaller magnification.
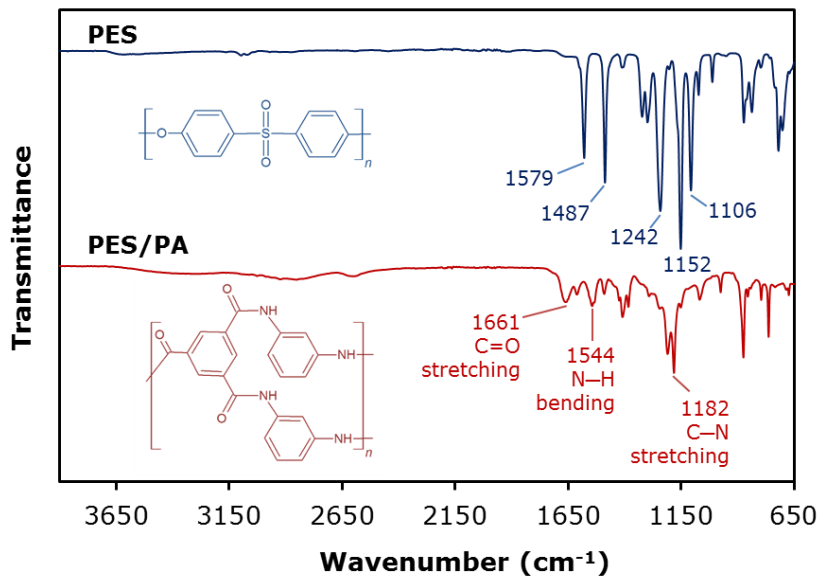
**Figure 2.** FTIR spectra of (a) PES membrane and (b) PA/PES membrane
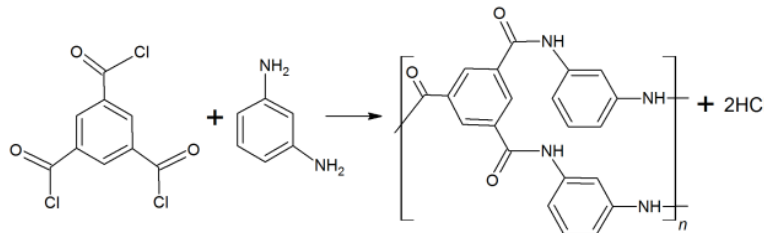
Figure 3. Interfacial polymerization reaction of MPD and TMC to form crosslinked polyamide

A peak is also observed at 1242 cm^{-1}, which can be attributed to the aromatic ether (Coates, 2006). Peaks representing sulfone group are found at 1152 cm^{-1} and 1106 cm^{-1} (Coates, 2006). The FTIR spectrum of PA/PES shows peaks at 1661 cm^{-1}, 1544 cm^{-1}, and 1182 cm^{-1}, confirming the presence of C=O stretching, N–H bending, and C–N stretching, respectively (Coates, 2006). The presence of these functional groups indicates the successful IP of MPD and TMC forming PA layer onto PES substrate (Figure 3). These results are in good agreement with other studies (Jun et al., 2019; Kamada et al., 2014). There is no peak detected in the wavenumber of 1725–1700 cm^{-1} indicating the presence of carboxylic acid groups (Mohamed et al., 2017), thus the structure of PA formed could be totally crosslinked units, which could be due to the high MPD/TMC ratio used (Jin and Su, 2009).

3.2. Surface Hydrophilicity

The hydrophilicity of pristine PES and PA/PES membrane surfaces, based on WCA measurement, were shown in Figure 4. In general, the membrane surface hydrophilicity decreased after IP of PA, indicated by increased WCA from 12.7° ± 3.3° to more than 50°. Increasing the concentration of TMC from 0.05 to 0.2 w/v.% then resulted in enhanced hydrophilicity, indicated by decreased WCA by about 16°. This enhanced hydrophilicity could be due to the increased portion of the hydrophilic linear structure with carboxylic acid groups (–COOH) in the PA layer as the MPD/TMC ratio decreases (Tian et al., 2013). Besides, since surface roughness is one of the parameters affecting surface wettability (Himma et al., 2017; Himma et al., 2018), the high WCA at the high MPD/TMC ratio could also be associated with its high surface roughness that causes more air trapped in the ridge-and-valley surface morphology and then reduces the contact area between membrane surface and water droplet. Meanwhile, the WCA on PA/PVDF membrane was not much different from the pristine PVDF membrane, which could be due to the loose PA layer formed as observed in the SEM image.
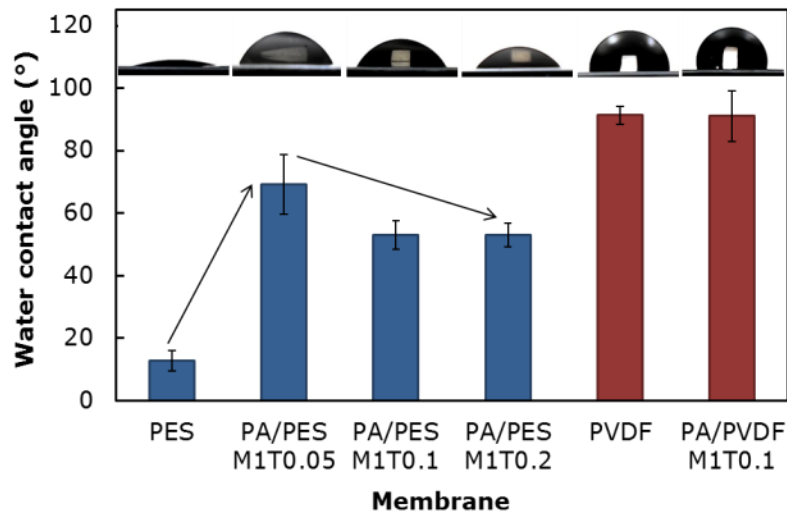
Figure 4. Water contact angle on the different membrane surfaces
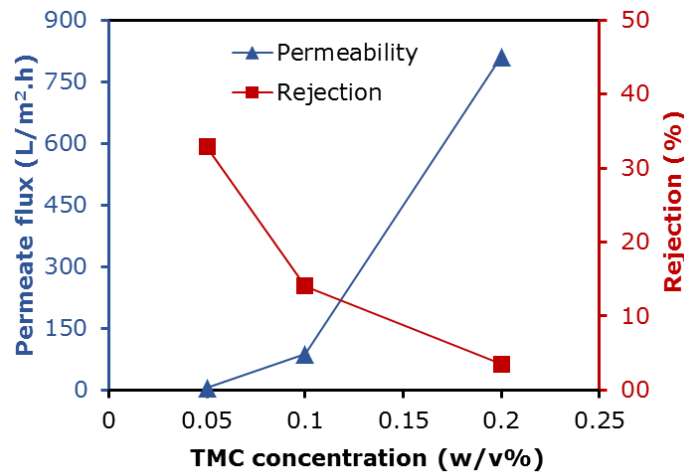
Figure 5. Permeate flux and sunset yellow rejection exhibited by PA/PES membranes in filtration at 3 bar and room temperature using dead-end flow configuration

In PA/PVDF membrane, the WCA values were spread out over a wide range, indicating inhomogeneity of the PA layer. Unexpectedly, higher WCAs were found in some locations across the PA/PVDF membrane, compared with the pristine membrane. This could be due to the increased surface roughness after the IP.
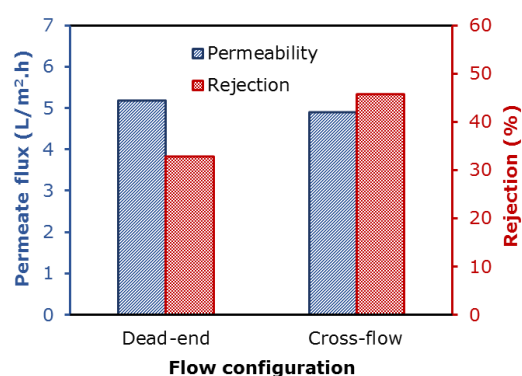
3.3. Separation Performance

Pure water flux measurements have been conducted for PES membrane and PA/PES M1T0.05 membrane. The results showed that the pure water flux of PA/PES M1T0.05 membrane was 12.59 ± 1.96° L/m².h, which was approximately 100% less than that of PES membrane, indicating the presence of dense layer in the PA/PES membrane. The performance of PA/PES membranes in sunset yellow removal is then shown in Figure 5. The increase of TMC concentration led to increased permeate flux but was accompanied by the decrease in sunset yellow rejection. This trend can be explained by the morphological changes in PA/PES membrane as discussed in the previous section. The increase in permeate flux could also be attributed to the enhanced hydrophilicity of the membrane surface, but this contribution seems to be small compared to that of change in PA layer density. This could be true since increasing TMC concentration from 0.1 to 0.2 w/v% resulted in almost no change in membrane hydrophilicity, but the permeate flux dramatically increased to 810.7 L/m².h accompanied by a high loss rejection to 3.5%.

Since the flow configuration is also another factor affecting the separation performance, cross-flow configuration was also conducted, compared with dead-end configuration, and

the results are depicted in Figure 6. Filtration with cross-flow configuration resulted in a slight decrease in permeate flux from 5.2 to 4.9 L/m^2.h but a significant improvement in rejection from 32.8 to 45.7%, compared to that with dead-end configuration. In the dead-end configuration, the feed is entirely forced through the membrane under pressure. The flow is in a normal direction to the membrane surface and the solutes are accumulated on the membrane surface. Meanwhile, in cross-flow configuration, the feed flows in a tangential direction to the membrane surface and a turbulent flow can be developed, preventing the rejected solutes from accumulating on the membrane surface.

Figure 6. Separation performance of PA/PES M1T0.05 membrane in filtration at 3 bar and room temperature using dead-end flow configuration.

The separation performance achieved by thin-film composite membranes in this work is relatively low compared to other works that also developed thin-film composite membrane for dye removal (Liu et al., 2017; Lü et al., 2019), in which high sunset yellow removal of more than 90% could be achieved. Liu et al., 2017 used piperazine as the monomer in the aqueous phase instead of MPD, applied heat treatment, and then modified the resulting thin-film composite membrane with diethanolamine. Meanwhile, in the study performed by Lü et al. (2019), the top layer could be more compact because of the secondary interface reaction using tannic acid. Thus, further optimization of process parameters or modification by incorporating other materials might be necessary to improve both flux and rejection in dye removal.

4. Conclusion

Thin-film composite membranes have been prepared by IP of MPD and TMC onto PES support membrane as well as PVDF support membrane. Homogeneous layer of PA was formed on the PES support but not on the PVDF support which could be due to the hydrophobicity of PVDF hindering the support wetting by MPD solution. Increasing MPD/TMC ratio by lowering TMC concentration resulted in enhanced PA layer density, leading to increased sunset yellow rejection which was accompanied by decreased permeate flux. Improved rejection of 45.7% was then obtained by using a cross-flow configuration. However, further development is highly needed to improve the membrane performance in dye removal.

Acknowledgement

References

Alenazi, N. A., Hussein, M. A., Alamry, K. A., Asiri, A. M. (2018) Nanocomposite-Based Aminated Polyethersulfone and Carboxylate Activated Carbon for Environmental Application. A Real Sample Analysis. *C*, 4(2) 30.

Coates, J. (2006) Interpretation of Infrared Spectra, A Practical Approach. *Encyclopedia of Analytical Chemistry*. John Wiley & Sons.

Collivignarelli, M. C., Abbà, A., Carnevale Miino, M., Damiani, S. (2019) Treatments for color removal from wastewater: State of the art. *Journal of Environmental Management*, 236, 727-745.

Esfandian, F., Peyravi, M., Ghoreyshi, A. A., Jahanshahi, M., Rad, A. S. (2017) Fabrication of TFC nanofiltration membranes via co-solvent assisted interfacial polymerization for lactose recovery. *Arabian Journal of Chemistry,* 12(8), 5325-5338.

Himma, N. F., Wardani, A. K., Wenten, I. G. (2017) Preparation of Superhydrophobic Polypropylene Membrane Using Dip-Coating Method: The Effects of Solution and Process Parameters. *Polymer-Plastics Technology and Engineering*, 56(2), 184-194.

Himma, N. F., Prasetya, N., Anisah, S., Wenten, I. G. (2018) Superhydrophobic membrane: progress in preparation and its separation properties. *Reviews in Chemical Engineering*, 35(2), 211-238.

Jin, Y., Su, Z. (2009) Effects of polymerization conditions on hydrophilic groups in aromatic polyamide thin films. *Journal of Membrane Science*, 330(1), 175-179.

Jun, B.-M., Yoon, Y., Park, C. M. (2019) Post-Treatment of Nanofiltration Polyamide Membrane through Alkali-Catalyzed Hydrolysis to Treat Dyes in Model Wastewater. *Water*, 11(8),1645.

Kamada, T., Ohara, T., Shintani, T., Tsuru, T. (2014) Optimizing the preparation of multi-layered polyamide membrane via the addition of a co-solvent. *Journal of Membrane Science*, 453, 489-497.

Katheresan, V., Kansedo, J., Lau, S. Y. (2018) Efficiency of various recent wastewater dye removal methods: A review. *Journal of Environmental Chemical Engineering*, 6(4), 4676-4697.

Kustiningsih, I., Restiani, R., Raharja, T., Hasna, A., Sari, D. K. (2020) Degradation of Methyl Violet Using TiO$_2$-Bayah Natural Zeolite Photocatalyst. *Jurnal Rekayasa Kimia dan Lingkungan*, 5(1), 10-20.

Liu, M., Chen, Q., Lu, K., Huang, W., Lü, Z., Zhou, C., Yu, S., Gao, C. (2017) High efficient removal of dyes from aqueous solution through nanofiltration using diethanolamine-modified polyamide thin-film composite membrane. *Separation and Purification Technology*, 173, 135-143.

Lü, Z., Hu, F., Li, H., Zhang, X., Yu, S., Liu, M., Gao, C. (2019) Composite nanofiltration membrane with asymmetric selective separation layer for enhanced separation efficiency to anionic dye aqueous solution. *Journal of Hazardous Materials*, 368, 436-443.

Mohamed, M. A., Jaafar, J., Ismail, A. F., Othman, M. H. D., Rahman, M. A. (2017). Chapter 1 - Fourier Transform Infrared (FTIR) Spectroscopy. In N. Hilal, A. F. Ismail, T. Matsuura, D. Oatley-Radcliffe (Eds.), *Membrane Characterization,* 3-29). Elsevier.

Mohammad, A. W., Teow, Y. H., Ang, W. L., Chung, Y. T., Oatley-Radcliffe, D. L., Hilal, N. (2015) Nanofiltration membranes review: Recent advances and future prospects. *Desalination*, 356, 226-254.

Park, S.-J., Kwon, S. J., Kwon, H.-E., Shin, M. G., Park, S.-H., Park, H., Park, Y.-I., Nam, S.-E., Lee, J.-H. (2018) Aromatic solvent-assisted interfacial polymerization to prepare high performance thin film composite reverse osmosis membranes based on hydrophilic supports. *Polymer*, 144, 159-167.

Paul, M., Jons, S. D. (2016) Chemistry and fabrication of polymeric nanofiltration membranes: A review. *Polymer*, 103, 417-456.

Samsami, S., Mohamadizaniani, M., Sarrafzadeh, M-H, Rene, E. R., Firoozbahr, M. (2020) Recent advances in the treatment of dye-containing wastewater from textile industries: Overview and perspectives. *Process Safety and Environmental Protection*, 143, 138-163.

Shen, L., Yang, Y., Zhao, J. Wang, X. (2016) High-performance nanofiltration membrane prepared by dopamine-assisted interfacial polymerization on PES nanofibrous scaffolds. *Desalination and Water Treatment*, 57(21), 9549-9557.

Tian, M., Qiu, C., Liao, Y., Chou, S., Wang, R. (2013) Preparation of polyamide thin film composite forward osmosis membranes using electrospun polyvinylidene fluoride (PVDF) nanofibers as substrates. *Separation and Purification Technology*, 118, 727-736.

Xie, W., Geise, G. M., Freeman, B. D., Lee, H.-S., Byun, G., McGrath, J. E. (2012) Polyamide interfacial composite membranes prepared from m-phenylene diamine, trimesoyl chloride and a new disulfonated diamine. *Journal of Membrane Science*, 403-404, 152-161.

Yan, W., Wang, Z., Zhao, S., Wang, J., Zhang, P., Cao, X. (2019) Combining co-solvent-optimized interfacial polymerization and protective coating-controlled chlorination for highly permeable reverse osmosis membranes with high rejection. *Journal of Membrane Science*, 572, 61-72.

Zhang, X., Liu, C., Yang, J., Zhu, C.-Y., Zhang, L., Xu, Z.-K. (2020) Nanofiltration membranes with hydrophobic microfiltration substrates for robust structure stability and high water

permeation flux. *Journal of Membrane Science*, 593, 117444.

Zhu, J., Yuan, S., Uliana, A., Hou, J., Li, J., Li, X., Tian, M., Chen, Y., Volodin, A., der Bruggen, B. V. (2018) High-flux thin film composite membranes for nanofiltration mediated by a rapid co-deposition of polydopamine/piperazine. *Journal of Membrane Science*, 554, 97-108.